RESEARCH ARTICLE-MECHANICAL ENGINEERING

Evaluation of Machinability and Recast Layer Analysis of Ferrous Clay Composite through Electric Discharge Machining Process

Shrikrushna B. Bhosale[1] · **Sumit Bhowmik[2]** · **Amitava Ray[3]**

Abstract

Recent developments in material science have concentrated not only on the improvement in mechanical properties, but also on the machinability that was difficult for system profiles. The present research explains the machinability assessment of the part of the sintered powder metallurgy using an electric discharge machining. The ferrous clay matrix preparations are constructed from iron–carbon–copper material and bentonite clay. The selected input parameters for the measurement of machinability are wt. % of clay, current (A), pulse on time (μs) and voltage (V), whereas the electrode wear rate, material removal rate and surface roughness (R_a) are considered as performance features. Results show that the performance parameters have been optimized at three different parametric conditions. Further, to obtain single optimum condition the hybrid GRA-TOPSOS methodology has been implemented for maximum MRR with minimum EWR and low surface roughness. The single optimum condition has been found at 5% clay, current 7 A, voltage 49 V and pulse on time 400 μs. The study of micro-structure and chemical composition of machined surfaces has been carried out using scanning electron microscopy with X-ray diffraction and energy-dispersive spectrometry analysis, respectively. The SEM exposes the less recast layer and micro-cracks during electrical discharge machining of ferrous clay composite.

Keywords Electrical discharge machining · Material removal rate · Electrode wear rate · Optimization · Ferrous clay composite · GRA-TOPSIS

1 Introduction

The favourable combinations of mixing metals and non-metals have key assets in the powder metallurgy (P/M) process. Powder metallurgy composites have been got substantial attention in the present composite domain owing to a high potential in decent strength, stress-free formability, near net shape manufacturing and economical cost com-pared to traditional alloys which impact on the developing requirement of advanced composites in various industries. The most widely employed ferrous P/M parts have been used for industrial applications such as gears, vehicle parts, marine parts, aviation and power tool components due to improved mechanical properties [1]. The P/M composites are having production steps which implicate the powder preparation, mixing followed by compaction and subsequent sintering at elevated temperature. The result of present investigation has industrial applications for powder metallurgical components. Generally lock and structural parts, automobile parts, machines components, gears, etc. are produced by powder metallurgical components and these required some secondary machining operations like threads, grooves, undercuts, holes, etc. Therefore, machinability study of P/M composites fascinates the attention of many researchers. Many factors like alloying elements, porosity, presence of hard particles and heterogeneous micro-structure cause difficulties in machining of P/M components [2–5]. The predominant machining operations common in P/M are mainly drilling (30%), turning, tapping and boring (25%), and oth-

✉ Amitava Ray
  amitavaray.siliguri@gmail.com

  Shrikrushna B. Bhosale
  shrikrushna82@gmail.com

  Sumit Bhowmik
  bhowmiksumit04@yahoo.co.in

[1] Department of Mechanical Engineering, SVERI's College of Engineering, Pandharpur, Maharashtra, India

[2] Department of Mechanical Engineering, National Institute of Technology, Silchar, Assam, India

[3] Jalpaiguri Govt. Engineering College, Jalpaiguri, West-Bengal, India

ers (milling, unconventional machining) to a minor extent. So there is a huge chance in the machinability study of powder metallurgy composites using unconventional machining processes. Several machining processes like abrasives and water jet machining, ultrasonic machining, laser machining, etc. have been deliberated for machining of composites in the contemporary centuries [5, 6]. Amongst them, electrical discharge machining (EDM) offers various advantages like no burr production, no force on material hardness, production of complex shapes, etc. In electric discharge machining, the discrete electrical releases (flashes) are generated between the workpiece and tool which lead to erosion of a tiny amount of material from a workpiece surface. [7–9]. The major problems have occurred in machining of P/M composites via an EDM process due to thermal conductivity of the workpiece material, porosity, low material rate, poor surface finish, recast layer, micro-cracks, undesirable phase transformations and non-uniform dispersion of atoms. However, many researchers have been continuously striving for the development of machining of advanced materials/composites via an EDM process for various industrial applications [8–12]. In EDM, the machinability of processes has been mainly measured, viz. MRR, EWR and R_a with cost effectiveness. The EDM process parameters like pulse on time, current, gap voltage and pulse off time along with recast layer have a significant effect on performance parameters like MRR, EWR and R_a. To study the parametric contribution, the performance analysis has been studied for composite materials in electric discharge machining using Taguchi's experimental design and neuro-grey methodology [13–15]. Further, some researchers have made an attempt for optimization of EDM process parameters through different techniques like response surface methodology (RSM) [15, 16], desirability-based multi-objective particle swarm optimization [17] central composite design and desirability approach [18], grey relational analysis and TOPSIS [19–23], GRA-PCA [24], ANOVA [25, 26], tool electrode analysis using surface alloying [27], multi-phasic simulation method [28], analysis of surface morphology using SEM [29–31], fuzzy TOPSIS [32], RSM and NSGA-II-based optimization [33], genetic algorithm [34], TGRA-based optimization [35]. Few researchers have studied the micro-hardness and effect of dielectric in EDM process and also made comparative analysis using different MCDM techniques [36, 37].

In this context, the machinability analysis of ferrous clay composites has been performed in the EDM process for assessing process parameters. The novelty of the present work lies in the addition of bentonite (organic) clay as a machinability enhancer in ferrous alloy as no one has made such attempt. To evaluate the significance of clay, the analysis of machinability characterizations have been carried out. The selected input parameters are wet. % of bentonite clay (P_c), current (I_p), gap voltage (V) and pulse on time

(μs), while the response parameters are electrode wear rate (EWR), material removal rate (MRR) and surface roughness (R_a). A Taguchi method has been applied to interpret an influence of the input variables on the response parameters of the EDM process. The high MRR, less EWR and low R_a have been predicted at different conditions using analysis of variance. Further, GRA-TOPSIS hybrid methodology was employed to accomplish the single optimum machining condition which satisfies the several response parameters in the EDM operation. To explore the influence of process parameters on the recast layer, the machined surface analysis has been carried out with scanning electron microscopy (SEM). Also, X-ray diffraction (XRD and energy-dispersive spectrometry (EDS) analysis has been carried out for the study of chemical composition of ferrous clay composite.

2 Materials and Methods

2.1 Sample Preparation

The sample specimens have been prepared using prealloyed iron powder, having 2% copper, 0.8% graphite 0.3% MnS and balance Fe, [38] in which the bentonite clay (aluminium silicate) has been added to move over a ferrous clay composite. The bentonite clay has been varied from 0 to 5% at the interval of 1%. The ferrous clay composites were prepared at room temperature using a mechanical press and then subsequently sintered for 90 min at 1200 ºC in meticulous N2/H2 (90:10) atmosphere to avoid the rusting [39].

2.2 Experimental Design

The design of experiments encompasses a suitable selection of input factors and their levels. As per literature, based on pilot experimentation and testing machine specifications the parameters have been selected as wt. % of clay (P_c), current (I_p), gap voltage (V) and pulse on time (μs). A mixed 3–6 level Taguchi design method has selected to determine optimum EDM process variables for maximum MRR and minimum EWR to the low R_a. Accordingly, total eighteen experimental trials have been scheduled as per the designated design. Table 1 presents the process variables with their levels and fixed parameters.

2.3 Experimental Procedure

To assess the machinability of ferrous clay composite using EDM process, all experiments were performed as per Taguchi's L_{18} array. The experiments have been carried out on an electric discharge machine using ф 10 mm copper tool. The experimental arrangement of EDM is demonstrated in Fig. 1.

The weight of the workpiece and copper tool has been taken before and after each experiment to estimate the MRR and EWR using Eqs. 1 and 2, respectively. The surface roughness of the machined surface has been measured using a surface tester. The measured MRR, EWR and Ra values are presented in Table 2 as response parameters.

$$MRR = \frac{W_b - W_a}{T} \qquad (1)$$

where W_b and W_a represent weight of workpiece before and after machining, respectively, T = time of machining.

$$EWR = \frac{W_{tb} - W_{ta}}{T} \qquad (2)$$

where W_{tb} and W_{ta} represent electrode weight before and after machining, respectively, and T = time of machining.

3 Result and Discussion

3.1 Effect of Clay on Mechanical Properties

The effect of bentonite clay on mechanical properties in powder metallurgical composite has been explained as the less

Table 1 Process variables with levels

Input factors	Levels
Wt. % of clay (P_c)	0, 1, 2, 3, 4, 5
Current (I_p)	3, 5, 7
Gap voltage (V)	48, 49, 50
Pulse on time (μs)	400, 500, 600
Fixed parameters	
Dielectric	Kerosene
Tool material	AC grade copper
Tool diameter	10 mm

porosity has been found with increased weight percentage of clay as clay particles lodge the secondary pores created by liquid phase heating of copper at the grain boundary and clay particles can act as porosity filler. The overall density, hardness and crushing strength of the ferrous clay composite have been found reduced with increased weight percentage of clay [39].

3.2 Process Parameters Contribution

The response parameter data have been analysed using a statistical method. The ANOVA and percentage contribution for process parameters are presented in Table 3. The P value of current is found lowest, i.e. 0.004 which shows most significant factor in machining. Further P values wt. % of clay and pulse on time are lower, respectively. The P value of voltage is more which confirms minor effect on machinability. It is observed that the current (I_p) has more effect on the MRR, EWR and R_a, i.e. 54%, 72% and 66%, respectively. The wt. % of clay has additional influence on MRR (24%) and R_a (20%) compared to EWR (1%). Pulse on time (μs) has nearly the same effect on MRR (19%) and EWR (20%). The voltage (V) has a negligible significant effect on MRR (3%), EWR (7%) and R_a (5%).

3.3 Parameters Interaction Effect

Different parameter interactions are illustrated in Fig. 2. The most of the interactions has been observed at wt. % of clay levels with remaining machining parameters. For current at 5A, the interactions are clubbed together. Similarly, interactions have been observed at 50 V voltage and 500 μs pulse on time which shows strong parameter interactions. For remaining, inputs like current and voltage interactions are found at 50 V for 3A and 5A only. Further, current and voltage with pulse on time, the interactions are observed for

Fig. 1 **a** Experimental arrangement of EDM. **b** Enlarged view of machining

(a)　　　　(b)
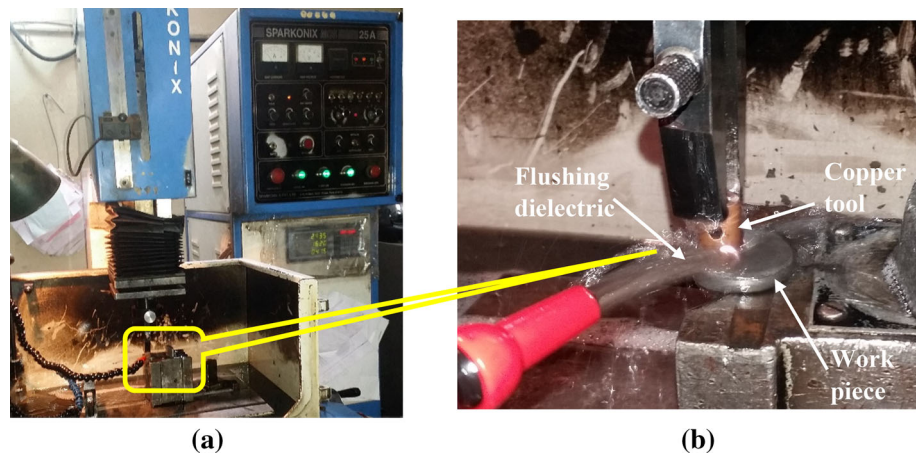
Table 2 Design matrix with actual values

Sr. no	Input factors				Performance measures		
	P_c (%)	I_p (A)	V	T_{on} (µs)	MRR (g/min)	EWR (g/min)	R_a (µm)
1	0	3	48	400	0.0744	0.0167	5.33
2	0	5	49	500	0.1239	0.0278	5.28
3	0	7	50	600	0.1239	0.0278	9.43
4	1	3	48	500	0.0563	0.0119	7.20
5	1	5	49	600	0.0986	0.0208	9.21
6	1	7	50	400	0.1315	0.0278	9.87
7	2	3	49	400	0.0598	0.0119	6.48
8	2	5	50	500	0.1047	0.0208	8.60
9	2	7	48	600	0.0698	0.0139	9.50
10	3	3	50	600	0.0492	0.0093	7.18
11	3	5	48	400	0.1106	0.0208	7.01
12	3	7	49	500	0.1475	0.0278	8.78
13	4	3	49	600	0.0520	0.0093	7.33
14	4	5	50	400	0.1559	0.0278	7.60
15	4	7	48	500	0.1169	0.0208	7.71
16	5	3	50	500	0.1157	0.0167	3.66
17	5	5	48	600	0.1446	0.0208	5.63
18	5	7	49	400	0.2893	0.0417	6.48

Table 3 ANOVA and percentage contribution

Source	DF	SS	MS	F	P	% Cont
Material removal rate (MRR)						
P_c	5	0.0198436	0.0039687	6.29	0.022	24%
I_p	2	0.0195337	0.0097669	15.47	0.004	54%
V	2	0.0032892	0.0016446	2.61	0.153	3%
T_{on}	2	0.0067132	0.0033566	5.32	0.047	19%
Error	6	0.0037872	0.0033566			
Total	17	0.0531668	0.0006312			
Electrode wear rate (EWR)						
P_c	5	0.0002247	0.0000449	5.30	0.033	1%
I_p	2	0.0006370	0.0003185	37.55	0.000	72%
V	2	0.0001059	0.0000530	6.24	0.034	7%
T_{on}	2	0.0001675	0.0000838	9.88	0.013	20%
Error	6	0.0000509	0.0000085			
Total	17	0.0011860				
Surface roughness (R_a)						
P_c	5	23.0369	4.6074	11.78	0.005	20%
I_p	2	17.8694	8.9347	22.84	0.002	66%
V	2	1.3764	0.6882	1.76	0.250	5%
T_{on}	2	4.5762	2.2881	5.85	0.039	9%
Error	6	2.3473	0.3912			
Total	17	49.2062				

Fig. 2 Parameter interaction effects
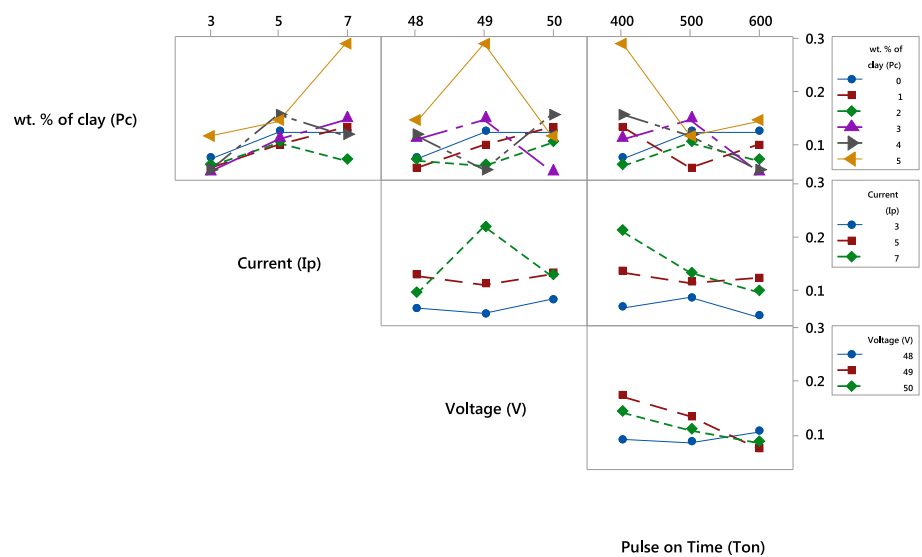
500 μs pulse on time for 3A and 5A and 600 μs pulse on time for 49 V and 50 V.

3.4 Means Analysis of MRR

The influence of process variables on material removal rate (MRR) is illustrated in Fig. 3. As the clay percentage increases when initially the material removal rate decreases, but after 2% clay MRR increases. The maximum MRR has been achieved at 5% clay. As less clay particles were coming in contact up to 2% clay, the less material removal rate was observed. Further, more clay particles have been released during machining resulting in an increase in MRR. Also, MRR has been increased as current increases and this phenomenon takes place due to thermal conductivity of clay. The more current produces more heat in the cutting zone due to which the material particles melt and vaporize. Finally, as pulse on time increases the MRR decreases due to heat spread through the specimen. To achieve the maximum MRR, 5% clay, 7 A current, 49 V and pulse on time 400 μs have been found beneficial.

3.5 Means Analysis of EWR

The effect of process variables on electrode wear rate (EWR) is demonstrated in Fig. 4 It has nearly the same graphical trend as MRR. As the clay percentage increases initially, the electrode wear rate decreases, but after 2% clay EWR increases. At less clay percentage (0%), the generated heat may erode the electrode resulting in high EWR. As a clay percentage increases, the more clay area may come in contact with heat and the generated heat has been utilized for EWR. Further, for small pulses on time, heat may not be transferred to composite but used for more EWR. At more pulse on time, the generated heat may properly transfer to composite results

with less EWR. For minimum EWR, 2% clay, 3 A current, 48 V and pulse on time 600 μs have benefitted.

3.6 Means Analysis of R_a

The influence of process variables on surface roughness (R_a) is shown in Fig. 5. The current and clay percentage has a major effect on surface roughness. As the current increases, the heat in the machining zone increases. This heat has been utilized to melt and vaporize the metal particles. After vaporization of metal particles, cavity formation takes place. These cavities may be filled with free clay resulting in a decrease in the surface roughness. More current resulted in high surface roughness due to melting and vaporization of metal particles and may be burning of free clay particles. The voltage and pulse on time have comparatively less influence on surface roughness (R_a). For low surface roughness, the 5% clay, 3 A current, 48 V and pulse on time 500 μs have benefitted.

From the above means analysis, it has been found that the current and clay percentage has a significant effect on MRR, EWR and R_a. Therefore, to achieve the maximum MRR, 5% clay, 7 A current, 49 V and pulse on time 400 μs have benefitted, and to obtain less EWR with low R_a, 2% clay, 3 A current, 48 V and pulse on time 600 μs and 5% clay, 3 A current, 48 V and pulse on time 500 μs have benefitted, respectively. This gives a different set of parameters for dissimilar response parameters. Each of these parameters has dissimilar measurement units for the criterion to quantify the performance of the process. Thus, the evaluation of the above performance parameters is not possible considering distinct measurement units. The GRA-TOPSIS methodology recommends a multiple response parametric optimization problem into a single response parameter optimization.
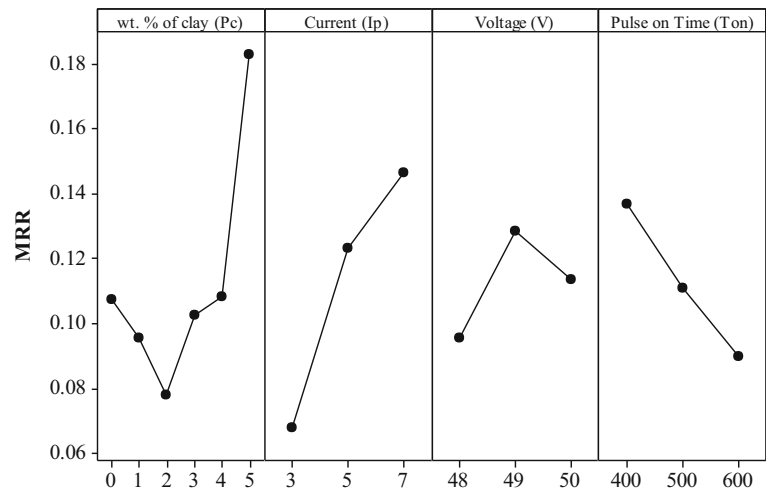
Fig. 3 Main effects plot for
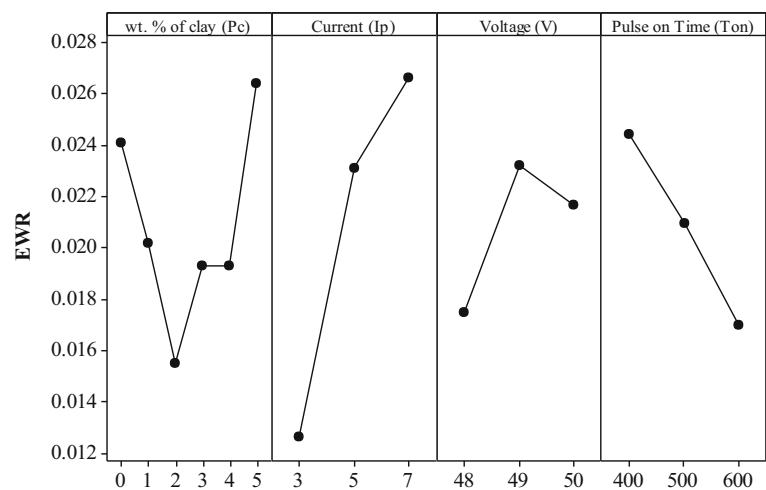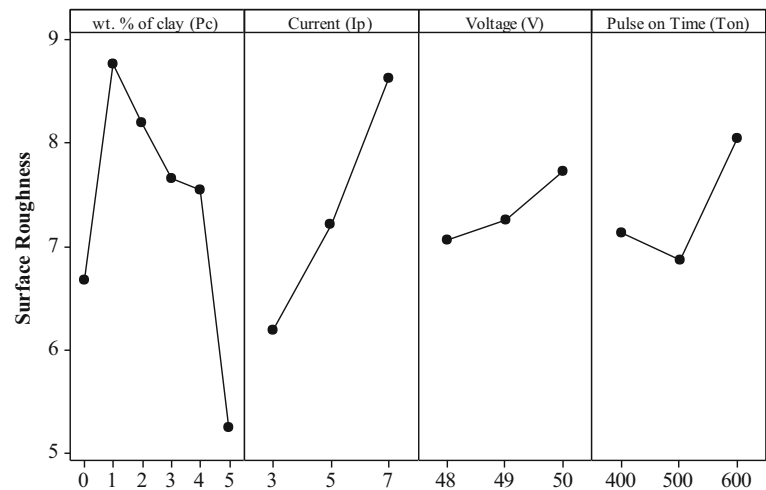MRR

Fig. 4 Main effects plot for
EWR

Fig. 5 Main effects plot for
surface roughness (Ra)

4 GRA-TOPSIS Methodology

In this segment, the GRA-TOPSIS decision-making model was anticipated to achieve a single process parameter optimal condition in the EDM process of ferrous clay composite. The

GRA-TOPSIS combined methodology has been projected which involves traditional steps of the primary methods. Initially, the experiments have been carried out as per the design of experiments to generate the decision matrix and then normalization of decision matrix has been performed according

Table 4 GRC values for all responses

Sr. no	Process parameters				GRC		
	P_c	I_p	V	T_{on}	MRR	EWR	R_a
1	0	3	48	400	0.275	0.591	0.552
2	0	5	49	500	0.330	0.366	0.559
3	0	7	50	600	0.330	0.366	0.262
4	1	3	48	500	0.259	0.804	0.367
5	1	5	49	600	0.300	0.482	0.270
6	1	7	50	400	0.341	0.366	0.248
7	2	3	49	400	0.262	0.804	0.421
8	2	5	50	500	0.307	0.482	0.293
9	2	7	48	600	0.271	0.699	0.260
10	3	3	50	600	0.254	1.000	0.368
11	3	5	48	400	0.314	0.482	0.379
12	3	7	49	500	0.365	0.366	0.286
13	4	3	49	600	0.256	1.000	0.359
14	4	5	50	400	0.380	0.366	0.342
15	4	7	48	500	0.321	0.482	0.336
16	5	3	50	500	0.320	0.591	1.000
17	5	5	48	600	0.361	0.482	0.510
18	5	7	49	400	0.999	0.248	0.421

Table 5 Separation of every substitute from the PIS and NIS with rank

Sr. no	Process parameters				S +	S-	S + + S-	Ci	Rank
	P_c	I_p	V	T_{on}					
1	0	3	48	400	0.8568	0.6081	1.4649	0.4151	14
2	0	5	49	500	0.7471	0.7764	1.5235	0.5096	10
3	0	7	50	600	0.6794	0.9765	1.6559	0.5897	5
4	1	3	48	500	0.9332	0.6640	1.5973	0.4157	13
5	1	5	49	600	0.7380	0.8977	1.6356	0.5488	6
6	1	7	50	400	0.6690	0.9880	1.6570	0.5962	3
7	2	3	49	400	0.9394	0.6123	1.5517	0.3946	15
8	2	5	50	500	0.7325	0.8790	1.6115	0.5455	7
9	2	7	48	600	0.8568	0.8003	1.6571	0.4830	12
10	3	3	50	600	1.0657	0.6331	1.6988	0.3727	17
11	3	5	48	400	0.7363	0.8117	1.5479	0.5243	9
12	3	7	49	500	0.6461	0.9620	1.6081	0.5982	2
13	4	3	49	600	1.0631	0.6426	1.7057	0.3767	16
14	4	5	50	400	0.6379	0.9229	1.5608	0.5913	4
15	4	7	48	500	0.7225	0.8458	1.5684	0.5393	8
16	5	3	50	500	1.0706	0.4143	1.4850	0.2790	18
17	5	5	48	600	0.7289	0.7216	1.4505	0.4975	11
18	5	7	49	400	0.1730	1.2073	1.3803	0.8747	1

to the category of quality features, i.e. the higher the better or the lower the better. The GRC values have been calculated from all the normalized response variables [19–22]. Then GRC has evaluated for all the response variables as given in Table 4.

Further, the GRC values have been considered in TOPSIS calculations. The standard methodology of the TOPSIS method has been explained by many researchers [22, 23]. The characteristics are: MRR, EWR and R_a. For the anticipated specific problem, MRR is considered as a beneficial characteristic (i.e. higher values), while EWR and R_a are considered as non-beneficial (i.e. smaller values) characteristics. Accordingly, the positive ideal solution (PIS) A + and negative ideal solution (NIS) A- have been calculated [23]. Finally, separation of every substitute from the positive ideal solution and negative ideal solution has been predicated to express the relative closeness of a particular alternative to the ideal solution. The comparative closeness to ideal solution is presented in Table 5.

From this, it has found that the setting of experiment 18 has the highest relative closeness performance index for higher MRR and less EWR with low R_a. Therefore, the process parameters set for experiment 18 have the optimal set of process parameters amongst the eighteen experiments. In other words, the optimum condition for higher MRR and less EWR with low R_a has been found at 5% clay, current 7 A, voltage 49 V and pulse on time 400 μs.

5 Surface Topography

5.1 X-ray diffraction (XRD) and energy-dispersive spectrometry (EDS) analysis

The X-ray diffraction (XRD) analysis of ferrous clay composite has been carried out by Ultima IV X-ray diffractometer, with Cu-Ka radiation operating at 40 kV, 40 mA. The three clamorous and robust echoes at 101 and 300 for 2ө° position which reveals the silicon dioxide, and at 110 for 2ө° position, the aluminium–iron has been observed for ferrous clay composite as shown in Fig. 6. The height of the peak increases with an increase in wt. % of clay. The nearly peak less conditions were observed at no clay condition. This shows the homogeneous mixing of clay in ferrous clay composite.

The energy-dispersive spectrometry (EDS) analysis has been carried out for study chemical composition of ferrous clay composite. The EDS analysis has been carried out for no clay, minimum clay (1%) and maximum clay (5%) condition which has been demonstrated in Fig. 7 for a, b and c, respectively. Figure 7a represents the EDS analysis of 0% clay sample in which Al and Si percentages have been found absent, while Fig. 7b represents EDS analysis of 1% clay wherein Al and Si percentages has found 1.64% and 1.67%, respectively. The increased Al and Si percentages have been noticed in the EDS analysis of 5% clay as shown in Fig. 7c

Fig. 6 XRD analysis at different wt. % of clay
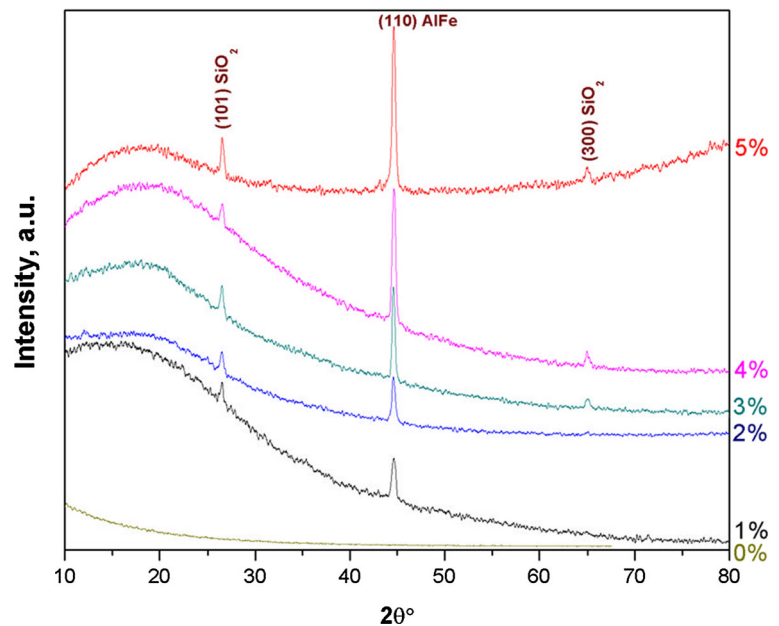
where it has been observed as 8.05% and 19.93%, respectively.

5.2 Scanning Electron Microscope (SEM) Analysis

The EDM machined surface of ferrous clay composite has been examined for analysing the influence of wt. % of clay by scanning electron microscopy (SEM). Also, as per ANOVA, as given in Table 3, the current has been found to be the most significant factor which contributes 54%, 72% and 66% for variation in MRR, EWR and R_a, respectively. Hence, the SEM has been carried out for the 0%, 1% and 5% clay samples as no clay, minimum clay and maximum clay percentage samples with combination with three levels of current (I_p), i.e. 3A, 5A and 7A.

Figure 8a, b and c shows the SEM analysis for 0% clay condition for 3A, 5A and 7A current, respectively. Figure 8a depicts some debris particles and micro-cracks on recast or white layer due to the less current. Further, Fig. 8b shows less debris particles as increased current resulted in more recast layers. In Fig. 8a, b, recast layer has observed in layer type formation due to less energy. At last Fig. 8c shows that debris particles and recast layers may get rewelded due increased energy of increased current. The continuous recast layer along with small debris particles is shown in Fig. 8c.

Figure 9a, b and c shows the SEM analysis for 1% clay condition for 3A, 5A and 7A current, respectively. Figure 9a depicts micro-holes on the recast layer due to the presence of less clay and less energy due to low current. Further, Fig. 9 (b) shows more gaps in the recast layer due to the presence of clay, but increased current resulted in the formation of the recast layer. At last, Fig. 9c shows that the more recast layer compared to Fig. 9a, b due to increased energy of increased current. In comparison with Fig. 8, in the presence of clay, the recast layer has found to be reduced.

Figure 10a, b and c shows the SEM analysis for 5% clay condition for 3A, 5A and 7A current, respectively. Figure 10a depicts a non-uniform recast layer due to the presence of more clay. Further, Fig. 10b shows debris or clay particles in the recast layer but, increased clay percentage resulted in the formation of less recast layer. At last, Fig. 10c demonstrates the negligible recast layer and clay particles may get surrounded by molten metal. This may be possible due to increased energy of increased current. In comparison with Figs. 8, 9, in the presence of clay, the recast layer has found to be more reduced.
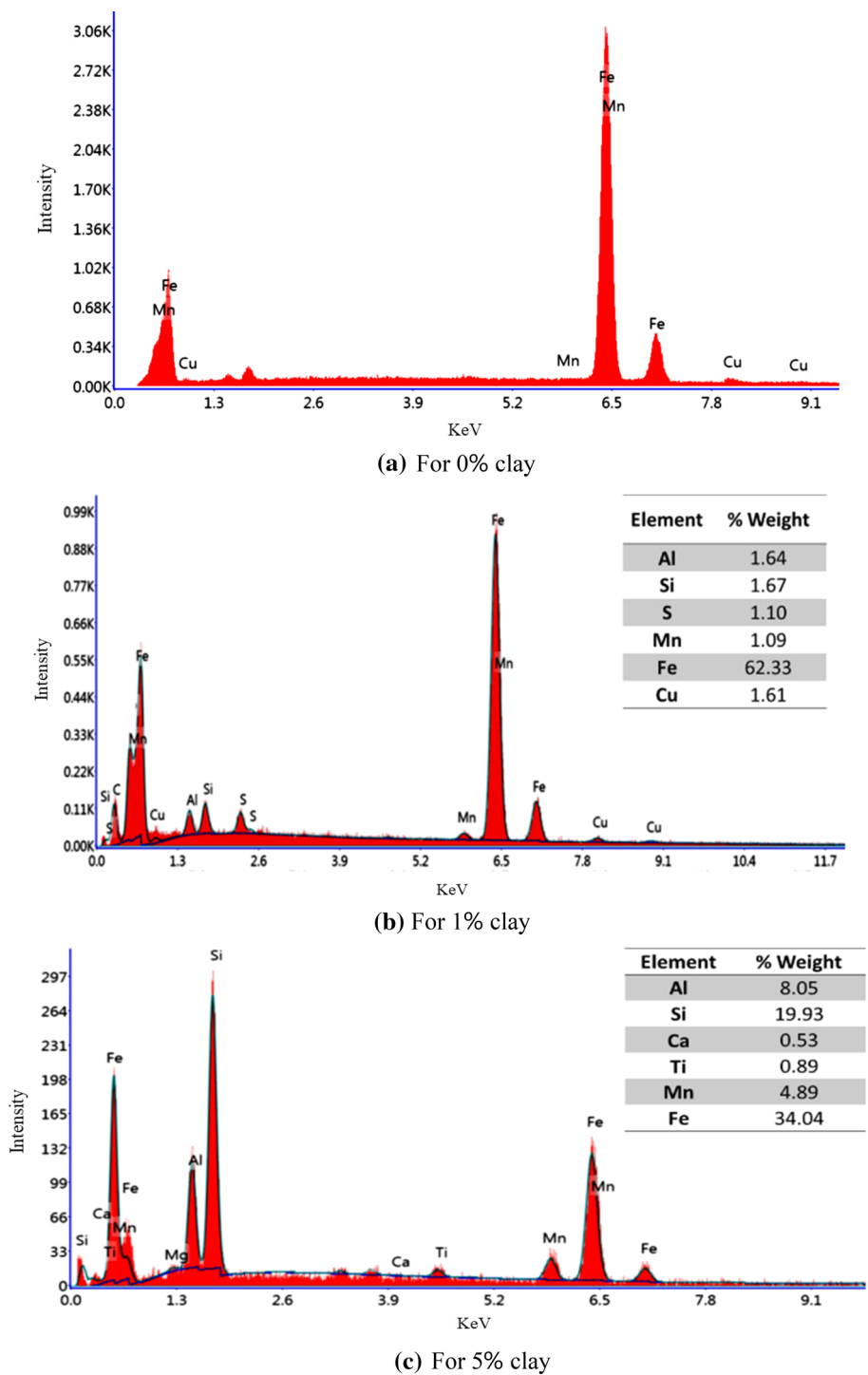
Therefore, more wet. % of clay resulted in the minimum recast layer formation, which has been favourable for the EDM process of ferrous clay composite.

6 Conclusions

The ferrous clay composite has been machined using the EDM process. The influence of EDM process variables on response parameters has been deliberated. The following conclusions can be exhausted from the above analysis-

1. From statistical analysis, the maximum MRR with less EWR and low R_a have been obtained at different parametric conditions. The maximum MRR at 5% clay, 7 A current, 49 V and pulse on time 400 μs, and less EWR, at 2% clay, 3 A current, 48 V and pulse on time 600 μs

Fig. 7 EDS analysis at different wt. % of clay

(a) For 0% clay

Element	% Weight
Al	1.64
Si	1.67
S	1.10
Mn	1.09
Fe	62.33
Cu	1.61

(b) For 1% clay

Element	% Weight
Al	8.05
Si	19.93
Ca	0.53
Ti	0.89
Mn	4.89
Fe	34.04

(c) For 5% clay

and low R_a at 5% clay, 3 A current, 48 V and pulse on time 500 μs have been found pre-eminently.

2. The current has a significant effect on the response parameters which contributes 54%, 72% and 66% for variation in MRR, EWR and R_a, respectively. The wt. % of clay has a second significant effect on MRR and R_a which contributes 24% and 20%, respectively. The wt. % of clay has negligible effect on EWR.

3. Using GRA-TOPSIS multi-objective optimization methodology, the single optimum condition for maximum MRR and less EWR with low R_a has been established at 5% clay, current 3 A, voltage 50 V and pulse on time 400 μs.

4. The X-ray diffraction reveals a homogeneous mixture of clay in ferrous clay composite. The energy-dispersive spectrometry (EDS) analysis shows the increased Al and

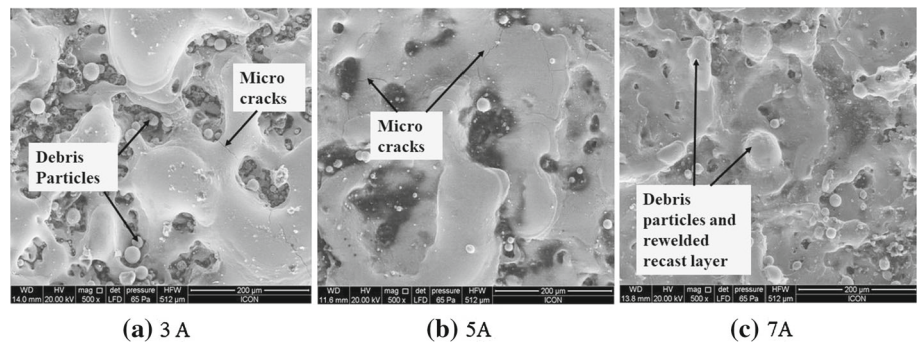**Fig. 8** SEM images for 0% clay at different current

(a) 3 A   **(b)** 5A   **(c)** 7A

Fig. 9 SEM images for 1% clay at different current

(a) 3 A   **(b)** 5A   **(c)** 7A
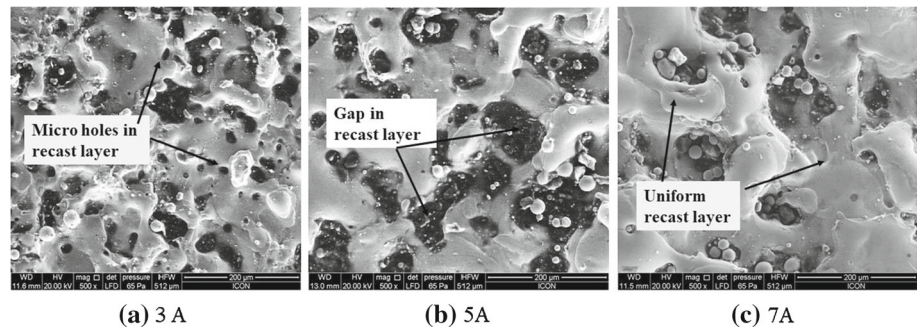
Fig. 10 SEM images for 5% clay at different current

(a) 3 A   **(b)** 5A   **(c)** 7A
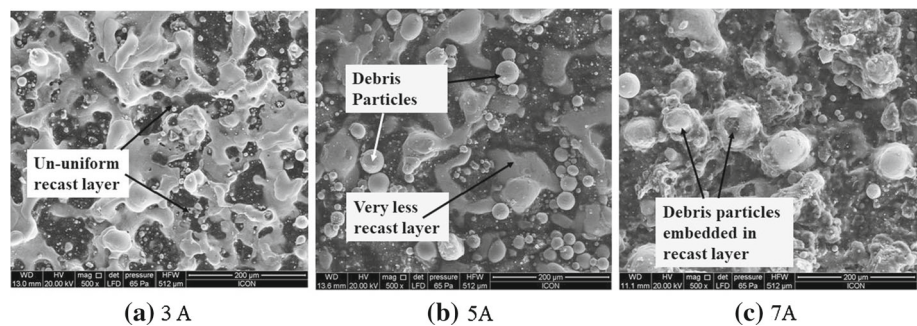
Si percentages with an increase in wt. % of clay in ferrous clay composite.

5. The SEM analysis illustrates that the addition of clay reduces the recast layer in the EDM process. More recast layers have been observed at no clay condition, while less recast layers have been witnessed at 5% clay condition.

References

1. Kandavel, T.K.; Chandramouli, R.; Karthikeyan, P.: Influence of alloying elements and density on aqueous corrosion behaviour of some sintered low alloy steels. Mater. Des. **40**, 336–342 (2012). https://doi.org/10.1016/j.matdes.2012.03.033

2. Blais, C.; L'Espérance, G.; Bourgeois, I.: Characterisation of machinability of sintered steels during drilling operations. Powder Metall. (2001). https://doi.org/10.1179/003258901666194

3. Park, J.; Lee, S.; Kang, S.; Jeon, J.; Lee, S.H.; Kim, H.; Choi, H.: Complex effects of alloy composition and porosity on the phase transformations and mechanical properties of powder metallurgy steels. Powder Technol. **284**, 459–466 (2015). https://doi.org/10.1016/j.powtec.2015.07.029

4. Bhosale, S.B.; Pawade, R.S.; Brahmankar, P.K.: Effect of process parameters on MRR, TWR and surface topography in ultrasonic machining of alumina-zirconia ceramic composite. Ceram. Int. **40**, 12831–12836 (2014). https://doi.org/10.1016/j.ceramint.2014.04.137

5. Tougas, B.; Blais, C.: Ultrasound-assisted drilling of copper and pre-alloyed powder metallurgy steels. Powder Metall. **60**, 49–55 (2017). https://doi.org/10.1080/00325899.2016.1273990

6. Salak, A.; Selecka, M.; Danninger, H.: Machinability of powder metallurgy steels. Cambridge International Science Publishing, Springer (2005)

7. Ferraris, E.; Reynaerts, D.; Lauwers, B.: Micro-EDM process investigation and comparison performance of Al 3O2 and ZrO2 based ceramic composites. CIRP Ann. - Manuf. Technol. **60**, 235–238 (2011). https://doi.org/10.1016/j.cirp.2011.03.131

8. Mohanty, C.P.; Mahapatra, S.S.; Singh, M.R.: An intelligent approach to optimize the EDM process parameters using utility concept and QPSO algorithm. Eng. Sci. Technol. an Int. J. **20**, 552–562 (2017). https://doi.org/10.1016/j.jestch.2016.07.003

9. Talla, G.; Sahoo, D.K.; Gangopadhyay, S.; Biswas, C.K.: Modeling and multi-objective optimization of powder mixed electric discharge machining process of aluminum/alumina metal matrix composite. Eng. Sci. Technol. an Int. J. **18**, 369–373 (2015). https://doi.org/10.1016/j.jestch.2015.01.007

10. Ugarteche, C.V.; Furlan, K.P.; Vale Pereira Do, R.; Trindade, G.; BinderBinderKlein, R.C.A.N.: Effect of microstructure on the thermal properties of sintered iron-copper composites. Mater. Res. (2015). https://doi.org/10.1590/1516-1439.030915

11. Bhuyan, R.K.; Mohanty, S.; Routara, B.C.: RSM and Fuzzy logic approaches for predicting the surface roughness during EDM of Al-SiCp MMC. Mater. Today: Proceed. **4**(2), 1947–1956 (2017)

12. Singh Sidhu, S.; Singh Bains, P.: Study of the recast layer of particulate reinforced metal matrix composites machined by EDM. Mater. Today Proc. **4**, 3243–3251 (2017). https://doi.org/10.1016/j.matpr.2017.02.210

13. Surya, V.R.; Kumar, K.M.V.; Keshavamurthy, R.; Ugrasen, G.; Ravindra, H.: Prediction of machining characteristics using artificial neural network in Wire EDM of Al7075 based In-situ composite. Mater. Today Proc. **4**, 203–212 (2017). https://doi.org/10.1016/j.matpr.2017.01.014

14. Gangil, M.; Pradhan, M.K.; Purohit, R.: Review on modelling and optimization of electrical discharge machining process using modern techniques. Mater Today: Proceed. **4**, 2048–2057 (2017)

15. Gopalakannan, S.; Senthilvelan, T.: Application of response surface method on machining of Al-SiC nano-composites. Meas. J. Int. Meas. Confed. (2013). https://doi.org/10.1016/j.measurement.2013.04.036

16. Dey, A.; Debnath, S.; Pandey, K.M.: Optimization of electrical discharge machining process parameters for Al6061/cenosphere composite using grey-based hybrid approach. Trans. Nonferrous Metals Soc. China **27**(5), 998–1010 (2017)

17. Majumder, A.: Process parameter optimization during EDM of AISI 316 LN stainless steel by using fuzzy based multi-objective PSO. J. Mech. Sci. Technol. (2013). https://doi.org/10.1007/s12206-013-0524-x

18. Gopalakannan, S.; Senthilvelan, T.: Optimization of machining parameters for EDM operations based on central composite design and desirability approach. J. Mech. Sci. Technol. (2014). https://doi.org/10.1007/s12206-013-1180-x

19. Manikandan, N.; Kumanan, S.; Sathiyanarayanan, C.: Multiple performance optimization of electrochemical drilling of inconel 625 using taguchi based grey relational analysis. Eng. Sci. Technol. an Int. J. (2017). https://doi.org/10.1016/j.jestch.2016.12.002

20. Naveen, B.; Anil S, K.M.; Sharma, C.: Optimisation of electrical discharge machining process with CuW powder metallurgy electrode using grey relation theory. J. Mach. Mach. Mater. **9**, 103–115 (2011)

21. Kumar, S.; V., Kumar. M, P.: Optimization of cryogenic cooled EDM process parameters using grey relational analysis. J. Mech. Sci. Technol. (2014). https://doi.org/10.1007/s12206-014-0840-9

22. Mishra, B.P.; Routara, B.C.: An experimental investigation and optimisation of performance characteristics in EDM of EN-24 alloy steel using Taguchi method and grey relational analysis. Mater. Today: Proceed. **4**, 7438–7447 (2017)

23. Manivannan, R.; Kumar, M.P.: Multi-response optimization of Micro-EDM process parameters on AISI304 steel using TOPSIS. J. Mech. Sci. Technol. (2016). https://doi.org/10.1007/s12206-015-1217-4

24. Jagadish, R.; A.: Optimization of process parameters of green electrical discharge machining using principal component analysis PCA. Int. J. Adv. Manuf. Technol. (2016). https://doi.org/10.1007/s00170-014-6372-8

25. Kao, J.Y.; Tsao, C.C.; Wang, S.S.; Hsu, C.Y.: Optimization of the EDM parameters on machining Ti-6Al-4V with multiple quality characteristics. Int. J. Adv. Manuf. Technol. (2010). https://doi.org/10.1007/s00170-009-2208-3

26. Selvarajan, L.; Sathiya Narayanan, C.; Jeyapaul, R.; Manohar, M.: Optimization of EDM process parameters in machining Si3N4-TiN conductive ceramic composites to improve form and orientation tolerances. Meas. J. Int. Meas. Confed. **92**, 114–129 (2016). https://doi.org/10.1016/j.measurement.2016.05.018

27. Gill, A.S.; Kumar, S.: Surface alloying by powder metallurgy tool electrode using EDM process. Mater. Today Proc. **2**, 1723–1730 (2015). https://doi.org/10.1016/j.matpr.2015.07.006

28. Hackert-Oschätzchen, M.; Paul, R.; Kowalick, M.; Kuhn, D.; Meichsner, G.; Zinecker, M.; Schubert, A.: Characterization of an electrochemical machining process for precise internal geometries by multiphysics simulation. Procedia CIRP. **58**, 175–180 (2017). https://doi.org/10.1016/j.procir.2017.04.021

29. Ashok kumarLaxminarayanaAravindan, U.P.N.: Study of surface morphology on micro machined surfaces of AISI 316 by Die Sinker EDM. Mater. Today Proc. **4**, 1285–1292 (2017). https://doi.org/10.1016/j.matpr.2017.01.149

30. Dewangan, S.; Gangopadhyay, S.; Biswas, C.K.: Study of surface integrity and dimensional accuracy in EDM using Fuzzy TOPSIS and sensitivity analysis. Meas. J. Int. Meas. Confed. (2015). https://doi.org/10.1016/j.measurement.2014.11.025

31. Lakshmanan, S.; Chinnakutti, P.; Namballa, M.K.; Engineering, M.; MC, a: Optimization of surface roughness using response surface methodology for EN31 tool steel EDM machining. Int. J. Recent Dev. Eng. Technol. **2**, 64–71 (2013)

32. Pattnaik, S.K., Priyadarshini, M., Mahapatra, K.D., Mishra, D., Panda, S. (2015) Multi objective optimization of EDM process parameters using fuzzy TOPSIS method. In: ICIIECS 2015 - 2015 IEEE International Conference on Innovations in Information, Embedded and Communication Systems

33. Khullar, V.R.; Sharma, N.; Kishore, S.; Sharma, R.: RSM- and NSGA-II-based multiple performance characteristics optimization of EDM parameters for AISI 5160. Arab. J. Sci. Eng. (2017). https://doi.org/10.1007/s13369-016-2399-5

34. Dilip, D.G.; Panda, S.; Mathew, J.: Characterization and parametric optimization of micro-hole surfaces in Micro-EDM drilling on inconel 718 super alloy using genetic algorithm. Arab. J. Sci. Eng. (2020). https://doi.org/10.1007/s13369-019-04325-4

35. Nguyen, P.H.; Banh, T.L.; Mashood, K.A.; Tran, D.Q.; Dong Pham, V.; Muthuramalingam, T.; Duc Nguyen, V.; Nguyen, D.T.: Application of TGRA-based optimisation for machinability of high-chromium tool steel in the EDM process. Arab. J. Sci. Eng. (2020). https://doi.org/10.1007/s13369-020-04456-z

36. Niamat, M.; Sarfraz, S.; Shehab, E.; Ismail, S.O.; Khalid, Q.S.: Experimental characterization of electrical discharge machining of aluminum 6061 T6 alloy using different dielectrics. Arab. J. Sci. Eng. (2019). https://doi.org/10.1007/s13369-019-03987-4

37. Sindhu, S.S.; Yazdani, M.: Comparative analysis of MCDM techniques for EDM of SiC/A359 composite. Arab. J. Sci. Eng. (2017). https://doi.org/10.1007/s13369-017-2726-5

38. Bhosale, S.B.; Bhowmik, S.; Ray, A.: Multi criteria decision making for selection of material composition for powder metallurgy process. Mater. Today: Proceed. **5**(2), 4615–4620 (2018). https://doi.org/10.1016/j.matpr.2017.12.032

39. Bhosale, S.B.; Bhowmik, S.; Ray, A.; A.: Experimental analysis and parametric optimization of drilling process for ferrous clay composite using GRA-PCA approach. J. Mate.r Res. Technol. **10**, 376–389 (2021). https://doi.org/10.1016/j.jmrt.2020.12.032